Diagnostic value of radial endobronchial ultrasonographic features in predominant solid peripheral pulmonary lesions

Xiaoxuan Zheng[1,2,3#], Lei Wang[4#], Jie Chen[4], Fangfang Xie[1,2,3], Yifeng Jiang[5], Jiayuan Sun[1,2,3]

[1]Department of Respiratory Endoscopy, Shanghai Chest Hospital, Shanghai Jiao Tong University, Shanghai, China; [2]Department of Respiratory and Critical Care Medicine, Shanghai Chest Hospital, Shanghai Jiao Tong University, Shanghai, China; [3]Shanghai Engineering Research Center of Respiratory Endoscopy, Shanghai, China; [4]Department of Ultrasound, Shanghai Chest Hospital, Shanghai Jiao Tong University, Shanghai, China; [5]Radiology Department, Shanghai Chest Hospital, Shanghai Jiao Tong University, Shanghai, China

Contributions: (I) Conception and design: J Sun; (II) Administrative support: J Sun, X Zheng, L Wang; (III) Provision of study materials or patients: All authors; (IV) Collection and assembly of data: All authors; (V) Data analysis and interpretation: X Zheng, L Wang, J Chen; (VI) Manuscript writing: All authors; (VII) Final approval of manuscript: All authors.

[#]These authors contributed equally to this work.

Correspondence to: Jiayuan Sun, PhD. Department of Respiratory Endoscopy and Department of Respiratory and Critical Care Medicine, Shanghai Chest Hospital, Shanghai Jiao Tong University, 241# West Huaihai Road, Shanghai 200030, China. Email: xkyyjysun@163.com.

Background: Transbronchial lung biopsy (TBLB) of peripheral pulmonary lesions (PPLs) is usually performed for a definite diagnosis. Radial probe endobronchial ultrasonography is often acknowledged as a good guidance method for TBLB as it can help physicians confirm the lesions' position. It is also a non-invasive imaging diagnostic method. This clinical study was designed to evaluate the ability of radial endobronchial ultrasonography (R-EBUS) to differentiate benign from malignant predominant solid PPLs based on imaging features.

Methods: Patients with predominant solid PPLs were enrolled in this study retrospectively. TBLB was performed using R-EBUS with or without other guidance techniques. One typical sonographic image and one video of each lesion were recorded for analysis. Six radial probe endobronchial ultrasonographic image features (size, shape, echogenicity, margin, blood vessel, and linear-discrete air bronchogram) were studied by ultrasonography specialists and physicians who were blinded to the final diagnosis. The sum score model of the combined predictive factors indicated the best diagnostic accuracies for predicting malignant PPLs. The model group results were used to establish the diagnostic standard for a verification group.

Results: A total of 303 patients were enrolled in the model group from July 2018 to July 2019 at the Shanghai Chest Hospital (214 with malignant and 89 with benign lesions). The mean lesion long axis on computed tomographic images was 34.39±13.79 mm. There were significant statistical differences between benign and malignant lesions in the long axis, short axis, shape, margin, blood vessel, and linear-discrete air bronchogram assessed by radial endobronchial ultrasound. Long axis, lobulation, distinct but not sharp margin, absence of blood vessel, and absence of linear-discrete air bronchogram were good predictive factors of malignant lesions. A sum score model value of 79.54% of these combined factors indicated the best diagnostic accuracy for predicting malignant lesions. Eighty-seven patients were enrolled in the verification group from August to October 2019. The sum score model showed a diagnostic accuracy of 82.76%.

Conclusions: Radial endobronchial ultrasonographic features can differentiate malignant from benign lesions and thus have potential diagnosis value in predominant solid PPLs.

Keywords: Transbronchial lung biopsy (TBLB); lung cancer; radial endobronchial ultrasonography imaging (R-EBUS imaging); peripheral pulmonary lesions (PPLs)

Introduction

Lung cancer is the leading cause of cancer mortality worldwide (1,2). Early diagnosis and treatment is important for a better prognosis. The increased frequency of high-quality computed tomography (CT) application allowed the identification of smaller pulmonary lesions at a larger rate than before (3,4). Peripheral pulmonary lesions (PPLs) can be diagnosed by transbronchial lung biopsy (TBLB), which has 36–88% sensitivity for detecting peripheral lung cancer (5). At present, PPLs diagnosis depends on histopathological evaluation, while the evidence on the utility of noninvasive ultrasonographic diagnosis is insufficient.

Radial endobronchial ultrasonography (R-EBUS) is usually acknowledged as a good guidance method for TBLB, helping physicians confirm the position of the lesions before taking a biopsy. The diagnostic yield of TBLB in patients with PPLs had significantly improved under R-EBUS guidance (6-9). R-EBUS is also a good diagnostic tool to distinguish benign from malignant diseases based on imaging features (10-12). Previous studies have shown a promising trend in the application of R-EBUS for PPLs diagnosis. However, their findings are difficult to apply in clinical practice because of the complex classification. Furthermore, a predictive model for PPLs diagnosis should be established. Besides, the clinical applicability of these R-EBUS image features needs confirmation by a verification study. Therefore, this study was designed to use a large number of R-EBUS images to differentiate benign from malignant lesions through a model group analysis. The resulting predictive model was then assessed on a verification group. We present the following article in accordance with the STARD reporting checklist (available at http://dx.doi.org/10.21037/jtd-2020-abpd-004).

Methods

Model group

Patients

Patients with PPLs who underwent EBUS-TBLB from July 2018 to July 2019 retrospectively at the Shanghai Chest Hospital were enrolled in the model group. Inclusion criteria included: (I) patients aged >18 years with PPLs that required pathological analysis; (II) the presence of a bronchus leading to or adjacent to the lesion on a chest CT scan. Exclusion criteria: (I) ground-glass opacity (GGO) of >50% of the lesion; (II) severe cardiopulmonary dysfunction and other indications that the patient cannot tolerate bronchoscopy; (III) lesion can be visualized by bronchoscopy; (IV) low quality of the ultrasonographic image record. There was no lesion size limit. The study was conducted in accordance with the Declaration of Helsinki (as revised in 2013). The Ethical Committee of Shanghai Chest Hospital approved this study (No. KS1709), and individual consent for this retrospective analysis was waived. The study was registered at the Clinical Trials Registry (identifier: NCT03575715).

TBLB procedure

Bronchoscopy was performed after inducing general anesthesia (propofol and remifentanil) by anesthesiologists or local anesthesia (lidocaine) by pulmonologists. R-EBUS was performed with an endoscopic ultrasonographic system (EU-ME2; Olympus, Tokyo, Japan), equipped with a 20-MHz mechanical radial type probe (UM-S20-17S or UM-S20-20R; Olympus). The R-EBUS probe was combined with or without other guidance equipment. When the bronchoscopist considered that the R-EBUS probe had reached the lesion, it was used to scan the lesion from its proximal to its distal end. A 10-second video was recorded, and a typical R-EBUS image was saved. The long and short axes of the lesion were measured at its maximum cross-section. After locating the PPL on the R-EBUS image, the probe was withdrawn. Brush or/and biopsy forceps were introduced through the working channel or guide sheath, and cytological and pathological specimens were obtained (13). No fewer than five biopsy specimens visible to the naked eye were obtained. We also obtained microbiological specimens if the bronchoscopist thought they were necessary.

R-EBUS imaging features

The R-EBUS images and videos were analyzed independently by two experienced doctors blinded to the final diagnosis after the TBLB procedure. Differences in results were discussed to determine the final result by consensus among three experts. This result was used for subsequent analysis.

According to our experience and that of others, lesions were characterized on the R-EBUS images based on the following features (*Figure 1*): (I) size—long and short axes; the long axis was the lesion's longest diameter at the maximum cross-section, while the diameter perpendicular to the long diameter at the maximum cross-section was
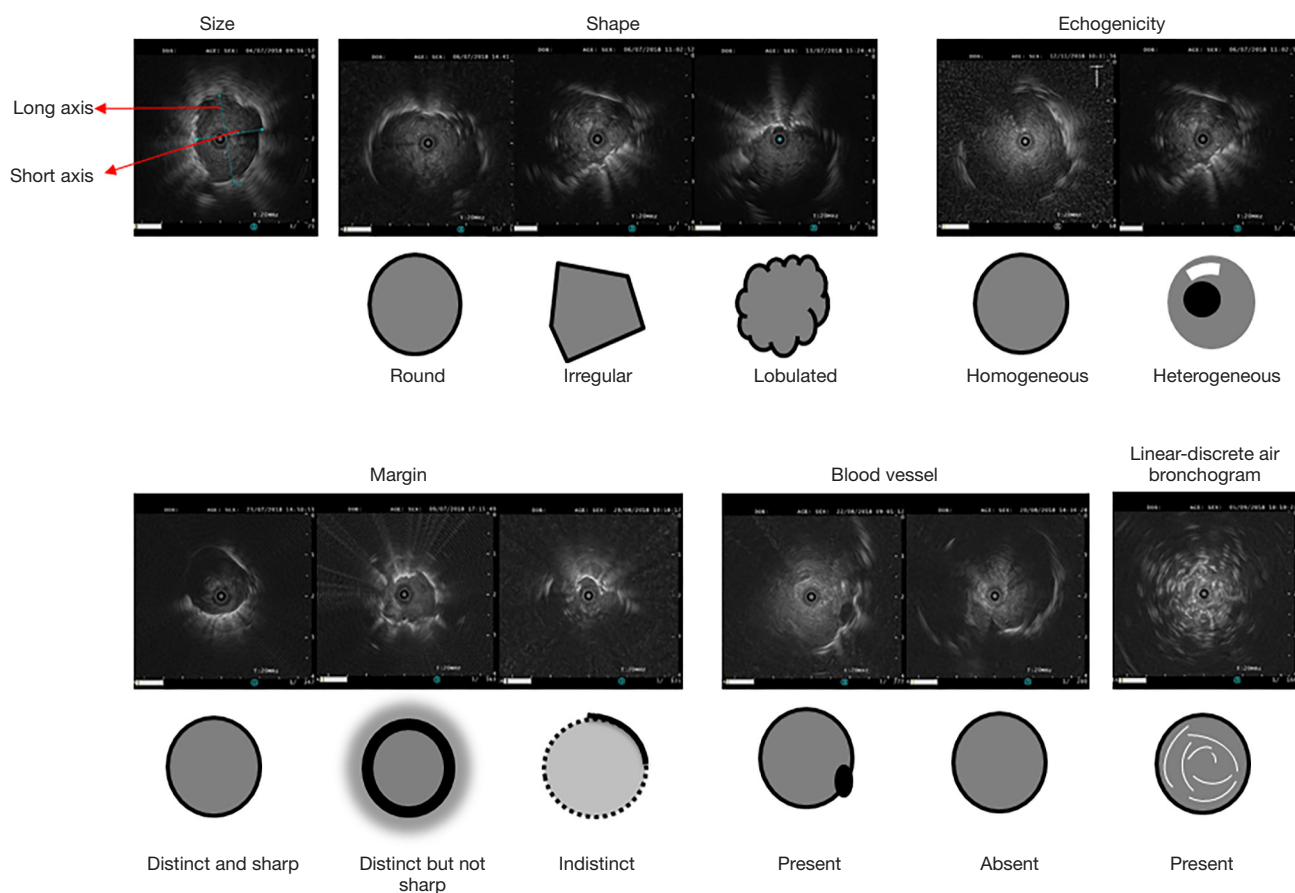
Figure 1 Representative morphologic features on endobronchial ultrasonographic images and analog diagrams used to classify malignant and benign lesions. Size: long and short axes; shape: round, irregular, or lobulated; echogenicity: homogeneous or heterogeneous; margin: distinct and sharp, distinct but not sharp, or indistinct; blood vessel: present or absent; linear-discrete air bronchogram: present or absent.

the short axis; (II) shape—round, irregular, or lobulated. Round lesions were defined as circular in shape with linear boundary and a long axis to short axis ratio smaller than 1.5; lobulation was defined as circular shape that had a changing boundary with a wave pattern; other lesions were defined as irregular (14); (III) echogenicity—the internal echo patterns were classified by morphology as homogeneous or heterogeneous (11,15); (IV) margin— when <50% of the margin was distinct, it was classified as indistinct margin; otherwise, it was classified as distinct margin. The distinct margin was subdivided into a sharp margin or a not sharp margin; a sharp margin was defined as a thin and clear margin, while any other margin was defined as not sharp margin (11); (V) blood vessel—present or absent blood vessels on the image (10,16); (VI) linear-discrete air bronchogram—laminar hyperechoic linear short lines with concentric alignment with a hypoechoic

background were divided based on whether the border was clear or not (12).

Diagnosis

Each histological and cytological specimen was interpreted separately by experienced pathologists. A definite histological diagnosis meant either malignant or typical benign pathology (17). If a lesion could not be diagnosed by bronchoscopy, we recommended other diagnostic procedures, including transthoracic needle aspiration, surgery, or other methods. If an undiagnosed patient refused further intervention, follow-up was considered as the second step. The final diagnosis was established by pathological evidence from biopsies taken during bronchoscopy or other invasive procedures, microbiological assessment, or clinical follow-up. All undiagnosed patients were followed up clinically for at least one year.

Table 1 Final diagnosis

Diagnosis	Model group (n=303)	Verification group (n=87)
Benign	89	27
Tuberculosis	14	2
Inflammation	68	24
Fungal infection	7	1
Malignant	214	60
Adenocarcinoma	149	43
Squamous cell carcinoma	17	8
Non-small cell carcinoma	10	5
Small cell carcinoma	5	1
Unknown type lung cancer	28	2
Neuroendocrine tumor	1	0
Hematological malignancies	3	1
Metastatic tumor	1	0

Verification group

Patients who underwent EBUS-TBLB at our institute from August to October 2019 were enrolled in the verification group. The inclusion and exclusion criteria, TBLB procedure, R-EBUS imaging features, and diagnostic criteria of the verification group were the same as in the model group. The appropriate predictive sonographic features were selected after analyzing the results of the model group. Three experienced doctors who were blinded to the final diagnosis predicted the type of the lesions using the R-EBUS features selected based on the model group after comparing the R-EBUS features during the TBLB procedure with the final diagnosis.

Statistical analyses

Patient characteristics were summarized using descriptive statistics for continuous variables (mean ± standard deviation) and frequency tables for categorical variables (numbers and percentages). Categorical variables were analyzed by chi-squared or Fisher's exact test, while continuous variables were analyzed by Student's t-test or Mann-Whitney U test. The inter-observer variability in the sonographic features was calculated by Cohen's kappa or Fleiss's methods. Sensitivity, specificity, accuracy, and positive and negative predictive values for the differential

diagnosis between benign and malignant lesions were calculated based on the final diagnosis (18). For this study, k values greater than 0.81 were considered to be in almost perfect agreement; 0.61–0.80 were considered substantial; 0.41–0.60, moderate; 0.21–0.40, fair; 0.00–0.20 slight agreement (19). A P value <0.05 was considered statistically significant. Univariate and multivariate analyses assessed the independent sonographic characteristics for predicting malignancy. ROC curve analysis was performed to analyze the diagnostic value of long axis and short axis. All statistical analyses were performed using IBM SPSS Statistics for Windows, Version 25.0 (IBM Corp., Armonk, NY, USA). We also calculated sum scores of positive criteria for malignant lesions to improve predictability.

Results

Baseline characteristics

A total of 303 patients were enrolled in the model group. There were 214 patients with malignant lesions (127 male and 87 female) and 89 with benign lesions (55 male and 34 female; *Table 1*). The mean long axis of the lesions on the CT images was 33.08±14.16 mm, and 21.48±8.75 mm on the R-EBUS images. The sex ratio was balanced (P=0.70). Total diagnostic yield by bronchoscopy was 71.3% (216/303), including 82.7% (177/214) for malignant lesions and 43.8% (39/89) for benign lesions. Based on the receiver-operating characteristic curve analysis of the model group, a short axis longer than 12.25 mm or a long axis longer than 17.75 mm had the highest sensitivity and specificity for predicting malignant lesions (*Figures 2* and *3*).

Sonographic features

Representative cases of benign and malignant were shown in *Figure 4*. Several R-EBUS features differed between benign and malignant lesions in the univariate analysis, including shape (P=3.24E-18), margin (P=9.88E-12), blood vessel (P=4.56E-07), and linear-discrete air bronchogram (P=1.81E-15). These factors also differed in the multivariate analysis (*Table 2*). The mean inter-observer agreement Kappa values for shape, margin, linear-discrete air bronchogram, echogenicity, and vessel were 0.920, 0.849, 0.979, 0.730, and 0.871, respectively.

Value of sonographic features for predicting malignancy

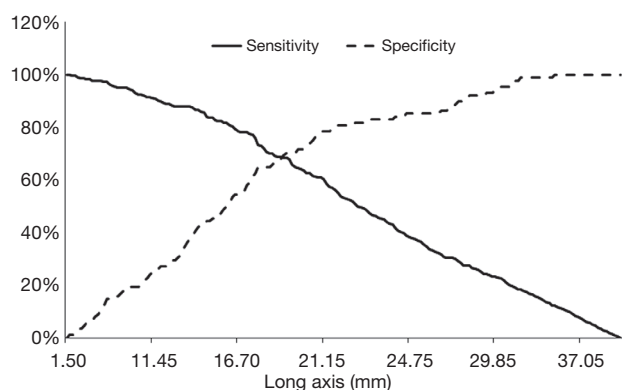We extracted four simplified imaging features for

Figure 2 Receiver-operating characteristic curve analysis for the long axis (mm). A threshold of 17.75 mm was determined to be the cutoff for telling malignant from benign lesions. A solid line indicates sensitivity; a dashed line indicates specificity.

Figure 3 Receiver-operating characteristic curve analysis for the short axis (mm). A threshold of 12.75 mm was determined to be the cutoff for telling malignant from benign lesions. A solid line indicates sensitivity; a dashed line indicates specificity.
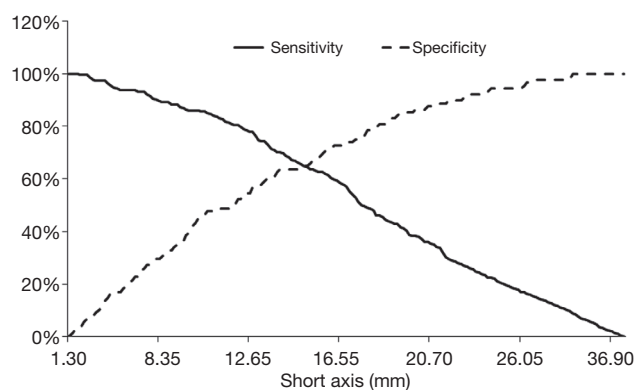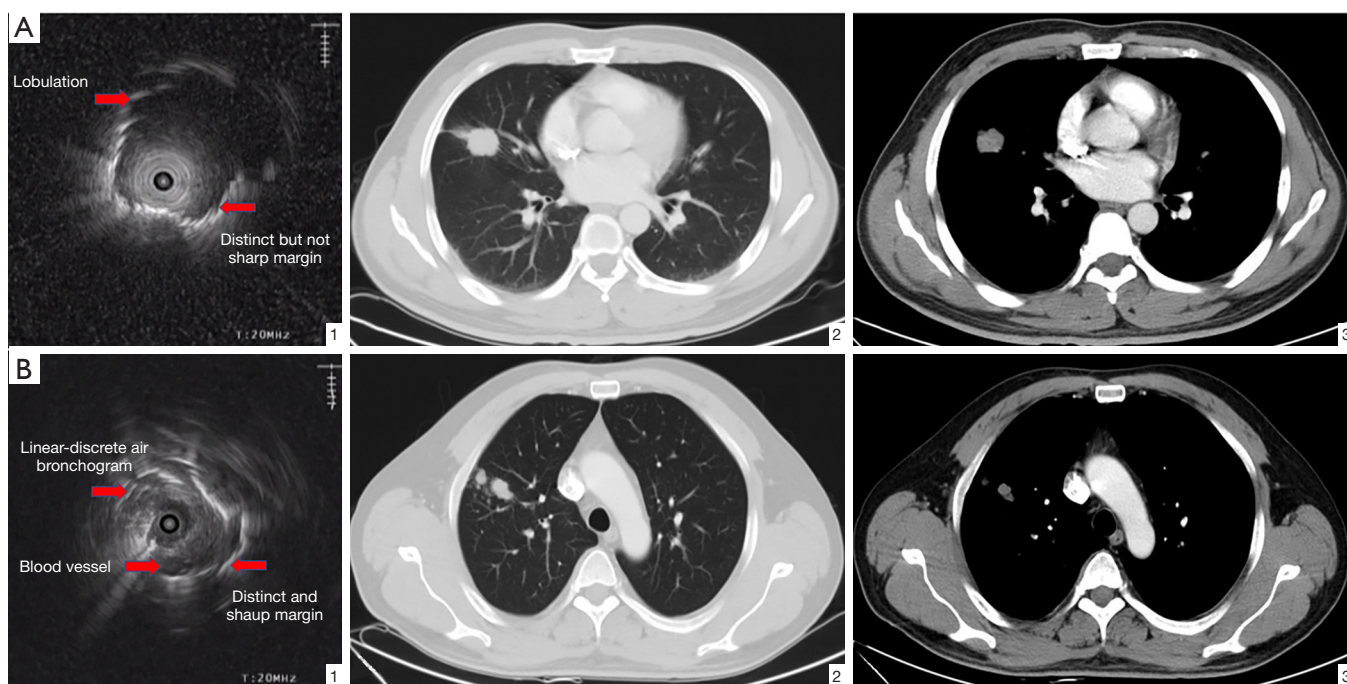

Figure 4 Representative cases of benign and malignant. (A1) Representative case of malignant lesion in radial endobronchial ultrasonographic features: lobulation, distinct but not sharp margin, absence of linear-discrete air bronchogram, absence of blood vessel. The sum score was 4. (A2,A3) Corresponding chest CT images of the malignant lesion. (B1) Representative case of benign lesion in radial endobronchial ultrasonographic features: irregular, distinct and sharp margin, linear-discrete air bronchogram, blood vessel. The sum score was 0. (B2,B3) Corresponding chest CT images of the benign lesion.

predicting malignancy based on the univariate and multivariate analyses: lobulation, distinct but not sharp margin, absence of blood vessel, and absence of a linear-discrete air bronchogram. The sensitivity, specificity, positive and negative predictive value, and diagnostic accuracy of these imaging features in identifying

Table 2 Univariate and multivariate analyses of radial endobronchial ultrasonographic features for predicting PPLs in model group

Ultrasonographic features	Covariate	Malignant (n=214)	Benign (n=89)	Total (n=303)	Ratio (malignant/ total) (%)	Univariate P value	Multivariate P value	Adjusted OR for positive (95% CI)
Long axis (mean ± SD, mm)		23.44±8.66	16.73±6.97	21.48±8.75		4.51E-10	4.83E-03	0.94 (0.89–0.98)
Short axis (mean ± SD, mm)		18.59±7.92	12.76±6.59	16.89±8.00		3.42E-09		
Shape	Round	10	23	33	30.30	3.24E-18	1.16E-05	7.81 (3.12–19.56)
	Irregular	56	53	109	51.38			
	Lobulated	148	13	161	91.93			
Echogenicity	Homogeneous	84	26	110	76.36	0.12		
	Heterogeneous	130	63	193	67.36			
Margin	Distinct and sharp	3	16	19	15.79	9.88E-12	4.40E-02	0.40 (0.16–0.98)
	Distinct but not sharp	162	34	196	82.65			
	Indistinct	49	39	88	55.68			
Blood vessel	Present	104	71	175	59.43	4.56E-07	8.33E-05	0.22 (0.10–0.47)
	Absent	110	18	128	85.94			
Linear-discrete air bronchogram	Present	45	62	107	42.06	1.81E-15	4.03E-07	0.15 (0.07–0.31)
	Absent	169	27	196	86.22			

PPLs, peripheral pulmonary lesions; SD, standard deviation.

malignancy are shown in *Table 3*.

A sum score model, in which the positive criteria were counted, was investigated to determine whether a combination of criteria would increase the detection accuracy of malignant lesions. The best sensitivity, specificity, positive and negative predictive values, and diagnostic accuracy values for predicting malignant lesions in PPLs with at least two of the four sonographic features (lobulation, distinct but not sharp margin, absence of blood vessel, and absence of linear-discrete air bronchogram) were 83.64%, 69.66%, 86.89%, 63.92%, and 79.54%, respectively (*Table 3*).

Verification group

A total of 87 patients (47 male and 40 female, P=0.82) were consecutively enrolled in the verification group (60 patients with malignant lesions and 27 with benign lesions). The mean long axis of the lesions on the CT images was 33.23±16.28 mm, and 22.39±7.48 mm on the R-EBUS images. The bronchoscopy diagnostic yield was 70.1%

(61/87), including 80% (48/60) in patients with malignant lesions and 48.1% (13/27) in patients with benign lesions. The sensitivity, specificity, positive and negative predictive values, and diagnostic accuracy for malignancy diagnosis in PPLs are shown in *Table 4*. The mean inter-observer agreement Kappa values of shape, margin, linear-discrete air bronchogram, echogenicity, and vessel were 0.748, 0.855, 0.779, 0.643, and 0.839, respectively. If we used the sum score model with at least two of the four sonographic features (lobulation, distinct but not sharp margin, absence of blood vessel, and absence of linear-discrete air bronchogram) to predict malignant lesions. The sensitivity, specificity, positive and negative predictive values, and diagnostic accuracy of this sum score model were 90.00%, 66.67%, 85.71%, 75.00%, and 82.76%, respectively.

Discussion

The results of this study indicated that four simplified sonographic features (lobulation, distinct but not sharp margin, absence of blood vessel, and absence of a linear

Table 3 Diagnostic test parameters and sum score system to predict PPLs in model group

Sonographic features	Sensitivity (%)	Specificity (%)	PPV (%)	NPV (%)	Acc (%)
Shape: lobulation	69.16	85.39	91.93	53.52	73.93
Margin: distinct but not sharp	75.70	61.80	82.65	51.40	71.62
Absence of linear-discrete air bronchogram	78.97	69.66	86.22	57.94	76.24
Absence of blood vessel	51.40	79.78	85.94	40.57	59.74
Sum score model					
None	7.01	65.17	32.61	22.57	24.09
1+	92.99	34.83	77.43	67.39	75.91
2+	83.64	69.66	86.89	63.92	79.54
3+	70.56	92.13	95.57	56.55	76.90
4	28.04	100.00	100.00	36.63	49.17

Sonographic features satisfy none (0) or at least one (1+), two (2+), three (3+), or four (4) of the four categories (lobulation, distinct but not sharp margin, absence of blood vessel and absence of linear-discrete air bronchogram). PPV, positive predictive value; NPV, negative predictive value; Acc, accuracy.

Table 4 Diagnostic test parameters and sum score system to predict PPLs in verification group

Sonographic features	Sensitivity (%)	Specificity (%)	PPV (%)	NPV (%)	Acc (%)
Shape: lobulation	80.00	92.59	96.00	67.57	83.91
Margin: distinct but not sharp	86.67	59.26	82.54	66.67	78.16
Absence of linear-discrete air bronchogram	75.00	74.07	86.54	57.14	74.71
Absence of blood vessel	61.67	77.78	86.05	47.73	66.67
Sum score model					
None	1.67	66.67	10.00	23.38	21.84
1+	98.33	48.15	76.62	90.00	78.16
2+	90.00	66.67	85.71	75.00	82.76
3+	76.67	92.59	95.83	64.10	81.61
4	35.00	100.00	100.00	40.91	55.17

Sonographic features satisfy none (0) or at least one (1+), two (2+), three (3+), or four (4) of the four categories (lobulation, distinct but not sharp margin, absence of blood vessel and absence of linear-discrete air bronchogram) based on model group. PPV, positive predictive value; NPV, negative predictive value; Acc, accuracy.

discrete air bronchogram) are useful tools for differentiating benign from malignant PPLs. The PPLs sum score model, with at least two of the four sonographic features, was a useful method to predict benign or malignant lesions. To our knowledge, this is the first large-sample R-EBUS image retrospective analysis and verification study.

Lung lesions continue to pose a diagnostic dilemma (20). When using R-EBUS images to assess PPLs, it is important for physicians to differentiate between benign and malignant

lesions as it might lead to a completely different treatment. For example, ten undiagnosed benign lesions (totally 14 undiagnosed benign lesions in the verification group) whose biopsy specimens were qualified had sum scores lower than two of the four malignant ultrasonographic features. These lesions might be truly negative. Clinical follow-up, including CT, was carried out in these patients. Eleven undiagnosed malignant lesions (totally 12 undiagnosed malignant lesions in the verification group) had sum

scores above the threshold in two of the ultrasonographic features. Their lesions were likely malignant according to the ultrasonographic features, but the pathological results were negative or biopsy specimen were unqualified. These results might be false negative, so another pathological examination was needed as soon as possible.

R-EBUS images permit visualization of the PPLs internal structure, providing valuable information to help with the differential diagnosis (8,21). Kurimoto *et al.* (10) devised a three-type and six-subtype classification system for distinguishing between benign and malignant lesions, and identifying the type of lung cancer. Based on this evidence, we developed a classification system with the aim of distinguishing between benign and malignant lesions more conveniently with a 20-MHz mechanical radial type ultrasonographic probe. Based on the four distinct characteristics on the R-EBUS images (lobulation, distinct but not sharp margin, absence of blood vessel, and absence of linear-discrete air bronchogram), it was easy to recognize the type when the threshold sum score was reached in at least two of the four sonographic features.

Some researchers think that heterogeneous internal echo is a characteristic of malignant lesions (11). Many malignant lesions in our study were a mixture of liquefying necrosis and GGO resulting in heterogeneous internal echo. However, heterogeneity in ultrasonographic images is also caused by linear-discrete air bronchogram and necrosis in benign lesions. Therefore, a judgment of ultrasonographic homogeneity is more subjective than the other imaging features and was found to be poor predictor in our study. Tumor lesions usually grow in an expansive and compressive manner, replacing the surrounding lung parenchyma. Thereafter, malignant lesions usually show lobulation, which is consistent with CT differentiation between benign and malignant lesions (14,22). Size is a factor for differentiating benign from malignant lesions. The depth and frequency should be adjusted during the R-EBUS procedure to achieve a comprehensive evaluation of very large lesions. The results of the study by Kuo *et al.* indicated that a continuous margin might be a useful tool for differentiating benign from malignant PPLs (12). In our study, we found that whether the margin was sharp could well distinguish benign from malignant lesions in the distinct margin group, in agreement with the CT and pathology results. Thin and clear borders are typical imaging features of benign lesions (23). Blood vessel structure was also an important feature for distinguishing benign from malignant lesions. We found no difference in the vessels within or adjacent to the lesions. Malignant lesions were harder than normal tissues or benign lesions, so they compressed small blood vessels. Therefore, we found fewer vessels in malignant lesions on the R-EBUS images than in benign ones. A linear-discrete air bronchogram suggested that tumor cells grew as a solid mass that replaced the lung parenchyma space, causing the laminar hyperechoic linear short lines to disappear (24).

Compared with single static images, we found the video to be more reliable when differentiating between benign and malignant lesions. Single static images are limited because they are taken based on the physician's personal opinion and depend on interference factors at the time. In contrast, a whole video can show lesions more completely and comprehensively. As far as we known, this is the first study based on R-EBUS videos and static images.

There are some limitations to this study. First, the data were retrospectively obtained from a single center. Second, the proportion of lesion types was unbalanced, potentially causing a bias in identifying benign and malignant lesions. Third, we excluded all pure GGO lesions to eliminate the influence of this factor. Therefore, the conclusions of this study cannot be applied to GGO. In the future, we will work with other hospitals to carry out multicenter prospective research to determine more comprehensive R-EBUS image features that can differentiate between PPL types. We hope to develop a quantitative index to analyze R-EBUS images to avoid the subjective bias in qualitative diagnosis (25-27), and maybe even use artificial intelligence neural network in the future (28). By that time, the prediction model will be more accurate, fast, objective, and non-invasive.

Conclusions

Our study supports utilizing R-EBUS imaging features to identify malignant lesions among PPLs. A prediction model that included lobulation, distinct but not sharp margin, absence of blood vessel, and absence of linear-discrete air bronchogram could help differentiate malignant from benign lesions in PPLs. R-EBUS image features might help in the diagnosis of predominant solid PPLs.

Acknowledgments

the Shanghai Municipal Health and Family Planning Commission (grant number 201640213).

Footnote

Provenance and Peer Review: This article was commissioned by the editorial office, *Journal of Thoracic Disease* for the series "Advance in Bronchoscopy for Peripheral Pulmonary Diseases". The article has undergone external peer review.

Reporting Checklist: The authors have completed the STARD reporting checklist. Available at http://dx. doi. org/10. 21037/jtd-2020-abpd-004

Data Sharing Statement: Available at http://dx. doi. org/10. 21037/jtd-2020-abpd-004

Conflicts of Interest: All authors have completed the ICMJE uniform disclosure form (available at http://dx. doi. org/10. 21037/jtd-2020-abpd-004). The series "Advance in Bronchoscopy for Peripheral Pulmonary Diseases" was commissioned by the editorial office without any funding or sponsorship. JS served as the unpaid Guest Editor of the series. The other authors have no other conflicts of interest to declare.

Ethical Statement: The authors are accountable for all aspects of the work in ensuring that questions related to the accuracy or integrity of any part of the work are appropriately investigated and resolved. The study was conducted in accordance with the Declaration of Helsinki (as revised in 2013). The Ethical Committee of Shanghai Chest Hospital approved this study (No. KS1709), and individual consent for this retrospective analysis was waived.

Open Access Statement: This is an Open Access article distributed in accordance with the Creative Commons Attribution-NonCommercial-NoDerivs 4.0 International License (CC BY-NC-ND 4.0), which permits the non-commercial replication and distribution of the article with the strict proviso that no changes or edits are made and the original work is properly cited (including links to both the formal publication through the relevant DOI and the license). See: https://creativecommons.org/licenses/by-nc-nd/4.0/.

References

1. Siegel RL, Miller KD, Jemal A. Cancer statistics, 2020. CA Cancer J Clin 2020;70:7-30.
2. Chen W, Zheng R, Baade PD, et al. Cancer statistics in China, 2015. CA Cancer J Clin 2016;66:115-32.
3. Aberle DR, Adams AM, Berg CD, et al. Reduced lung-cancer mortality with low-dose computed tomographic screening. N Engl J Med 2011;365:395-409.
4. Bach PB, Mirkin JN, Oliver TK, et al. Benefits and harms of CT screening for lung cancer: a systematic review. JAMA 2012;307:2418-29.
5. Rivera MP, Mehta AC, Wahidi MM. Establishing the diagnosis of lung cancer: Diagnosis and management of lung cancer, 3rd ed: American College of Chest Physicians evidence-based clinical practice guidelines. Chest 2013;143:e142S-65S.
6. Wang Memoli JS, Nietert PJ, Silvestri GA. Meta-analysis of Guided Bronchoscopy for the Evaluation of the Pulmonary Nodule. Chest 2012;142:385-93.
7. Andolfi M, Potenza R, Capozzi R, et al. The role of bronchoscopy in the diagnosis of early lung cancer: a review. J Thorac Dis 2016;8:3329-37.
8. Chen CH, Cheng WC, Wu BR, et al. Improved diagnostic yield of bronchoscopy in peripheral pulmonary lesions: combination of radial probe endobronchial ultrasound and rapid on-site evaluation. J Thorac Dis 2015;7:S418-25.
9. Ozgul G, Cetinkaya E, Ozgul MA, et al. Efficacy and safety of electromagnetic navigation bronchoscopy with or without radial endobronchial ultrasound for peripheral lung lesions. Endosc Ultrasound 2016;5:189-95.
10. Kurimoto N, Murayama M, Yoshioka S, et al. Analysis of the internal structure of peripheral pulmonary lesions using endobronchial ultrasonography. Chest 2002;122:1887-94.
11. Chao TY, Lie CH, Chung YH, et al. Differentiating peripheral pulmonary lesions based on images of endobronchial ultrasonography. Chest 2006;130:1191-7.
12. Kuo CH, Lin SM, Chen HC, et al. Diagnosis of peripheral lung cancer with three echoic features via endobronchial ultrasound. Chest 2007;132:922-9.
13. Zhang L, Wu H, Wang G. Endobronchial ultrasonography using a guide sheath technique for diagnosis of peripheral pulmonary lesions. Endosc Ultrasound 2017;6:292-9.
14. Li F, Sone S, Abe H, et al. Malignant versus benign nodules at CT screening for lung cancer: comparison of thin-section CT findings. Radiology 2004;233:793-8.
15. Lie CH, Chao TY, Chung YH, et al. New image characteristics in endobronchial ultrasonography for differentiating peripheral pulmonary lesions. Ultrasound Med Biol 2009;35:376-81.
16. Nishii Y, Yasuma T, Ito K, et al. Factors leading to

failure to diagnose pulmonary malignant tumors using endobronchial ultrasound with guide sheath within the target lesion. Respir Res 2019;20:207.

17. Ishida T, Asano F, Yamazaki K, et al. Virtual bronchoscopic navigation combined with endobronchial ultrasound to diagnose small peripheral pulmonary lesions: a randomised trial. Thorax 2011;66:1072-7.

18. Sun J, Zheng X, Mao X, et al. Endobronchial Ultrasound Elastography for Evaluation of Intrathoracic Lymph Nodes: A Pilot Study. Respiration 2017;93:327-38.

19. Garcia-Olivé I, Radua J, Serra P, et al. Intra- and interobserver agreement among bronchial endosonographers for the description of intrathoracic lymph nodes. Ultrasound Med Biol 2012;38:1163-8.

20. Schuhmann M, Eberhardt R, Herth FJ. Endobronchial ultrasound for peripheral lesions: a review. Endosc Ultrasound 2013;2:3-6.

21. Kurimoto N, Miyazawa T, Okimasa S, et al. Endobronchial ultrasonography using a guide sheath increases the ability to diagnose peripheral pulmonary lesions endoscopically. Chest 2004;126:959-65.

22. Pasnik M, Bestry I, Roszkowski-Sliz K. Solitary pulmonary nodule - the role of imaging in the diagnostic process. Adv Respir Med 2017;85:345-51.

23. Lee SM, Park CM, Goo JM, et al. Invasive pulmonary adenocarcinomas versus preinvasive lesions appearing as ground-glass nodules: differentiation by using CT features. Radiology 2013;268:265-73.

24. Izumo T, Sasada S, Chavez C, et al. Radial endobronchial ultrasound images for ground-glass opacity pulmonary lesions. Eur Respir J 2015;45:1661-8.

25. Morikawa K, Kurimoto N, Inoue T, et al. Histogram-based quantitative evaluation of endobronchial ultrasonography images of peripheral pulmonary lesion. Respiration 2015;89:148-54.

26. Nguyen P, Bashirzadeh F, Hundloe J, et al. Grey scale texture analysis of endobronchial ultrasound mini probe images for prediction of benign or malignant aetiology. Respirology 2015;20:960-6.

27. Badiei A, Nguyen P, Jersmann H, et al. Radial Endobronchial Ultrasound Greyscale Texture Analysis Using Whole-Lesion Analysis Can Characterise Benign and Malignant Lesions without Region-of-Interest Selection Bias. Respiration 2019;97:78-83.

28. Chen CH, Lee YW, Huang YS, et al. Computer-aided diagnosis of endobronchial ultrasound images using convolutional neural network. Comput Methods Programs Biomed 2019;177:175-82.